

Gulf Stream Marine Hydrokinetic Energy Off Cape Hatteras, North Carolina

AUTHORS

Michael Muglia
East Carolina University Coastal
Studies Institute

Harvey Seim
University of North Carolina—
Chapel Hill

Patterson Taylor
ECA Coastal Studies Institute

Introduction

Detailed observations of velocity structure, salinity, and temperature in the Gulf Stream (GS) off Cape Hatteras, NC, are analyzed to quantify spatial and temporal variability and inform marine hydrokinetic energy (MHK) development. The observations are part of the North Carolina Renewable Ocean Energy Program's (NCROEP) (General Assembly of North Carolina, 2012) focus on MHK in the GS. We characterize the variability in the energy resource from the GS current and the average power available, describe the shear profile, and investigate the susceptibility to turbulent mixing along the Cape Hatteras Line shown in Figure 1 as well as introduce some recent physical insights that are relevant to MHK objectives.

Background: Physical Oceanography

The GS, the subtropical western boundary current of the North Atlantic that transports the largest volume of water close to the U.S. seaboard, makes its closest approach to the coastline off eastern Florida and off

ABSTRACT

Multi-year measurements of current velocity, salinity, and temperature from fixed and vessel-mounted sensors quantify Gulf Stream (GS) marine hydrokinetic energy (MHK) resource variability and inform development off Cape Hatteras, NC. Vessel transects across the GS demonstrate a jet-like velocity structure with speeds exceeding 2.5 m/s at the surface, persistent horizontal shear throughout the jet, and strongest vertical shears within the cyclonic shear zone. Persistent equatorward flow at the base of the GS associated with the Deep Western Boundary Current (DWBC) produces a local maximum in vertical shear where stratification is weak and is postulated to be a site of strong turbulent mixing. Repeated transects at the same location demonstrate that the velocity structure depends upon whether the GS abuts the shelf slope or is offshore.

Currents from a fixed acoustic Doppler current profiler (ADCP) deployed on the shoreward side of the GS exceed 1 m/s 64% of the time 40 m below the surface. The 3.75-year time series of currents from the ADCP mooring document large, roughly weekly variations in downstream and cross-stream speed (−0.5 to 2.5 m/s) and shear ($\pm 0.05 \text{ s}^{-1}$) over the entire water column due to passage of GS meanders and frontal eddies. Current reversals from the mean GS direction occur several times a month, and longer period variations in GS offshore position can result in reduced currents for weeks at a time. Unresolved small-scale shear is postulated to contribute significantly to turbulent mixing.

Keywords: western boundary current, Gulf Stream, marine hydrokinetic energy

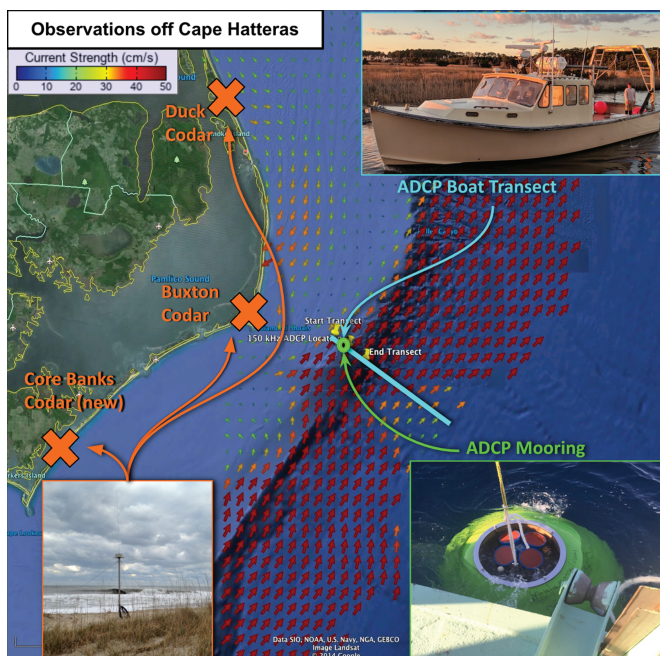
North Carolina (Miller, 1994). Off Cape Hatteras, GS velocities in the jet approach 3 m/s in the top 100 m of the water column, and volume transport estimates vary between 54.5 Sv (Heiderich & Todd, 2020) and 90 Sv ($1 \text{ Sv} = 1 \times 10^6 \text{ m}^3/\text{s}$) (Hogg, 1992). A complex confluence of several different water masses occurs in this region, from convergent shelf water masses (Flagg et al., 2002) and from the intersection of the Deep Western Boundary Current (DWBC) with the GS at greater depths (Andres et al., 2017).

GS structure between Cape Hatteras and 55°W has been studied extensively in multiple field experiments (Halkin &

Rosby, 1985; Hall & Bryden, 1985; Hogg, 1991; Meinen et al., 2009; Watts et al., 1995). The baroclinic structure of sloping isopycnals on the shoreward side of the GS, as well as horizontal and vertical scales, is thought to remain quite consistent in this area (Johns et al., 1995), notably maintaining structural consistency despite regular variations in GS position. A GS “wiggly garden hose” analogy was provided in Halkin and Rosby (1985), which refers to the stream structure being relatively consistent at their “Pegasus Line” north of Cape Hatteras between $35^\circ 13'$ and $36^\circ 27'$ despite varying regularly in position. Measured currents east of Cape Hatteras

FIGURE 1

Observation focus area off Cape Hatteras, NC, along the “Cape Hatteras Line” (cyan line across the GS) at $\sim 35^\circ\text{N}$. Orange Xs mark coastal ocean radar locations that produce the hourly averaged surface current measurements shown by arrows in the background where hotter colors represent faster currents, and three yellow push pins indicate the beginning of small vessel transects to measure currents, mooring location to measure currents, and offshore extent of small vessel transect, respectively. Transects currently extend ~ 70 km offshore from the 100-m isobath, to the eastern edge of the GS where currents are less than 50 cm/s. The green circle is the location of the 150-kHz ADCP mooring shown in the insert.



1994). Downstream of the Cape Hat-
 teras Line, the stream separates from
 the continental margin. Essentially un-
 constrained by bottom topography, me-
 ander variance doubles every 50 km,
 with the most energetic meanders hav-
 ing wavelengths of 180–460 km with
 periods of 4–100 days (Andres et al.,
 2016; Tracey & Watts, 1986). Thus,
 although the Cape Hatteras Line
 may be an optimal place for energy
 extraction because of its proximity
 to land and access to swift currents
 in relatively shallow water, these
 long-term measurements are essential
 because they are in a location not pre-
 viously observed by other extended
 studies.

Background: GS MHK

MHK is an often-used industry
 term that refers to the kinetic energy
 available from the marine environment.
 Some examples include energy from
 boundary currents, waves, and tidal cur-
 rents. Preliminary results from region-
 specific models indicate that variability
 in GS position is the main cause of vari-
 ability in the available MHK resource at
 a given location. Observations and
 model estimates at the acoustic Doppler
 current profiler (ADCP) mooring site in
 Figure 1 suggest the 271-day average
 power density is 798 and 641 W/m^2 ,
 respectively, 75 m below the surface
 between August 1, 2013, and April
 28, 2014. Annual model power densi-
 ty estimates at different locations along
 the ~ 70 km Cape Hatteras Line at a
 depth of 75 m vary from ~ 10 to nearly
 1,200 W/m^2 (Lowcher et al., 2014).
 The marked variability in power den-
 sity at a given location from year to
 year accentuates the importance of loca-
 tion consideration for GS MHK har-
 vesting and the annual variability at a
 single location. The power densities
 along the Cape Hatteras Line are like

those found in other western boundary currents such as the Agulhas, Brazil, and Kuroshio, which range from 0.5 to 2.0 kW/m² (Bane et al., 2017).

The observations presented herein identify several vital engineering considerations required for turbine and mooring design along the Cape Hatteras Line. Strong onshore flow and frequent flow reversals that occur with meander troughs suggest a turbine will be required to withstand multidirectional flow. The enhanced current resource closer to the ocean surface implies turbines will have to be engineered to prevent damage from surface waves. Strong shears at depth and unresolved small-scale shears that enhance the shear profile (Winkel et al., 2002) will demonstrate significant mooring design challenges.

The GS edge is, on average, 40 km offshore of Cape Hatteras based on U.S. Navy frontal analysis charts (Miller, 1994). The relatively small variability in stream position, resource proximity to land, and access to high current velocities in relatively shallow water have made the Cape Hatteras Line the focus of the NCROEP observation and modeling efforts to explore the potential for harvesting energy from the GS.

Observations

GS observations for the NCROEP began in 2013. Several different types of long-term consistent measurements have been made off of Cape Hatteras, NC (Figure 1): hourly surface currents from a land-based HF radar network, moored current measurements spanning nearly the entire water column from a 150-kHz ADCP at 35.14° north latitude and 75.11° west longitude in water 226 m deep, several cross-stream current velocity measure-

ments from vessel-mounted ADCPs, and water conductivity temperature depth (CTD) measurements from fixed-point moorings and vessel casts throughout the water column that characterize different water masses present. The observations reveal the GS flow field helps determine the skill of an existing Mid-Atlantic Bight/South Atlantic Bight Regional Ocean Model (Chen & He, 2010) in estimating the temporal and spatial variability of the GS resource and elucidate the engineering challenges inherent in turbine and mooring deployment for energy extraction from the GS. This manuscript presents observations from CTDs and ADCPs that were both moored and vessel mounted.

Current Velocity Measurements and CTD Casts From Vessels

Shipboard current measurements and CTD casts on a cross-stream section have been gathered as weather and vessel opportunity allowed, since 2013. The vessel measurements provide information about the GS velocity structure, the variability in MHK energy with water depth and location, and baroclinic structure near 35° north latitude. Early velocity measurements along a 14-km-long cross-stream/cross-isobath transect were collected with a downward-looking Teledyne 300-kHz Sentinel ADCP mounted on a small vessel. The transect intersected the moored ADCP location and spanned isobaths from 100 to 1,000 m in depth. The small vessel measures currents in the top 100 m of the water column with 1-m vertical resolution, with the shallowest current measurement 7 m below the surface. Qualitatively, measurements compared well with the moored ADCP current observations where they over-

lapped in space and time with good agreement in the current velocity structure from both instruments.

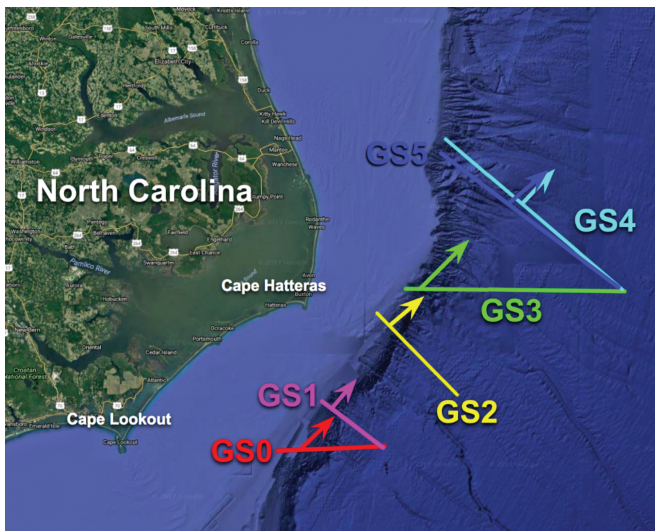
In 2016, we extended our measurements on the Cape Hatteras Line across the GS into the offshore anticyclonic shear zone where GS current speeds were less than 1 m/s, a distance of ~70 km, on the *R/V Armstrong*'s first Science Verification Cruise (SVC1). Later, as part of a larger National Science Foundation project—Processes driving Exchange At Cape Hatteras (PEACH), we explored several cross-stream transects (Figure 2) using the same vessel.

The *R/V Armstrong* has three hull-mounted Teledyne RDI ADCPs—300, 150, and 38 kHz with vertical resolutions of 2, 5, and 20 m, respectively. All vessel-mounted ADCP current velocity measurements were made absolute by using ancillary systems to measure vessel heading, velocity, pitch, and roll and remove them from measurements. The vessel also has a rosette sampler with a Seabird 911 CTD capable of making full water column casts at stations along the transects with processed data returned at 1-m vertical resolution. Current measurements made during casts, while the vessel was not underway, are of poor quality and not used for analysis. Deep CTD casts, below 1,600 m, take multiple hours to complete. Thus, the velocity and shear profiles at the cast location were estimated using the average of the current measurements made immediately preceding and following the cast.

In 2017, we outfitted the 42' vessel *Miss Caroline* to continue to make 70-km GS crossings along the Cape Hatteras Line (GS2 in Figure 2) measuring currents to depths in excess of 400 m using hull-mounted 300- and 75-kHz ADCPs, with 2- and 16-m

FIGURE 2

Large vessel cross-stream current transects made in April 2017 at six different locations off Cape Hatteras, NC. Currents were measured to water depths of 1,500 m along these transects. Figures below use the labels given on this figure. Arrows indicate the downstream direction chosen to be the direction of the maximum velocity vector.



resolution, respectively. We have made three GS crossings along GS2 on February 20, February 27, and August 31, 2018, with the new vessel and continue to do so. Additionally, a Seabird thermosalinograph continuously measures (1 Hz) surface temperature and salinity along the ship track. Presently, these measurements are planned to continue as long as funding for them is available.

Methods

150-kHz ADCP and CTD Mooring GS Transect Current Measurements and CTD Casts From Vessels

We have maintained a mooring on the upper slope in water depths of ~230 m since August 1, 2013 (Figure 1). The mooring contains a 150-kHz Teledyne Sentinel ADCP, Seabird SBE 37SM CTD, and Multi-Electronique passive acoustic hydrophone. Initially, it was recovered and replaced every 6–9 months. More recently, we have recovered and replaced the mooring annually, taking advantage of favorable summer weather. The ADCP measures currents with 4-m vertical resolution

(y) was that of the maximum velocity vector over the transect, taken to be the direction of the GS jet. The depth of the maximum velocity vector on the Cape Hatteras Line used in subsequent analysis was 13 m. The cross-stream direction (x) selected is positive clockwise perpendicular to the downstream direction or nearly cross-isobath offshore.

Vertical and cross-stream shears in downstream velocity (v) with depth and cross-stream distance, v/z and v/x , respectively, were derived. The resolutions of the vertical shear measurements presented are the same as individual ADCP velocity resolutions: 2, 5, and 20 m for 300, 150, and 38 kHz, respectively. The horizontal resolution is approximately 3.7 ± 1.3 km, estimated from the average vessel speed. The white curves running offshore in Figure 3 identify different ADCP coverage from the 300-kHz ADCP near the surface to the deepest coverage from the 38-kHz ADCP. Example velocity profiles from each ADCP at the CTD cast location are shown in Figure 4A.

From the ADCP velocities at the CTD cast (Figure 4B), the shear squared profile, where u is the cross-stream velocity, v is the downstream velocity, and z is the water depth, is determined.

$$S^2 = \left(\frac{\partial u}{\partial z} \right)^2 + \left(\frac{\partial v}{\partial z} \right)^2$$

The CTD cast is used to quantify the density stratification in the water column. To do so, the potential density was calculated from the salinity, temperature, and depth measurements made on the cast. From the potential density “ ρ ” profile, we calculate the buoyancy frequency squared, N^2 , that

FIGURE 3

From left to right: downstream velocity, shear with depth (vertical shear, $\partial v/\partial z$), and shear with cross-stream distance (horizontal shear, $\partial v/\partial x$). The vertical black line denotes the location of the analyzed CTD cast, from surface to bottom, and white curves delineate measurements made by each of three ADCPs—300, 150, and 38 kHz, respectively.

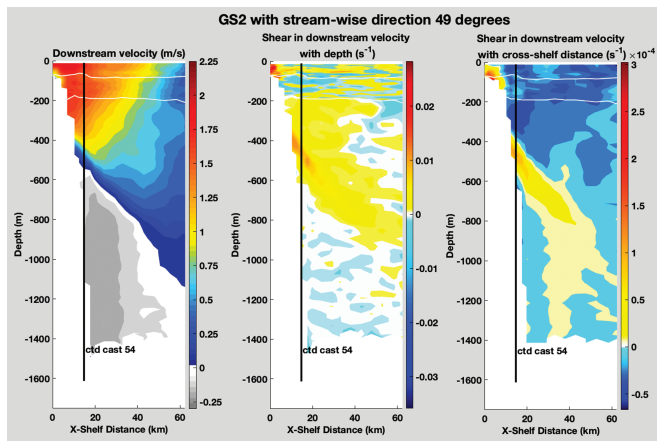
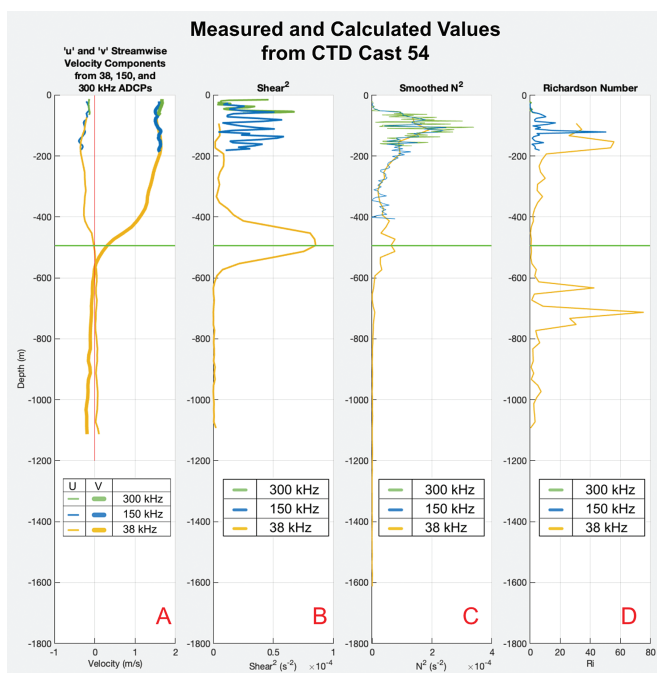


FIGURE 4

(A) The downstream “ v ” and cross stream “ u ” velocity components measured from the Armstrong’s 38-, 150-, and 300-kHz ADCPs at the CTD 54 cast location at 35.0720°N, 75.0230°W. The water depth at the cast is 1,613 m, as shown in Figure 3. (B) Profiles of the shear squared derived directly from the cast 54 velocity measurements in Figure 3 from each ADCP. (C) Smoothed profiles of the buoyancy frequency squared derived directly from the potential density measured on CTD cast 54 (Figure 3). (D) Richardson number profile derived from ADCP velocity measurements and CTD 54 cast. The bright green horizontal line marks the depth where mixing occurs between the GS and the DWBC—visible in Figure 3 along the CTD cast 54 line.



characterizes the stratification of the water column such that

$$N^2 = \frac{-g}{\rho} \frac{\partial \rho}{\partial z}$$

where g is the local acceleration due to gravity. N^2 was then smoothed to the resolution of each ADCP, namely, 2, 5, and 20 m, by convolving salinity and temperature used for density derivations from the CTD cast with 4-, 10-, and 40-point Bartlett windows, respectively (Figure 4C), to use in further analysis with the S^2 profiles from each ADCP with those resolutions.

To assess susceptibility to shear instabilities where the shears are high, the Richardson number, Ri , was calculated.

$$Ri = \frac{N^2}{S^2}$$

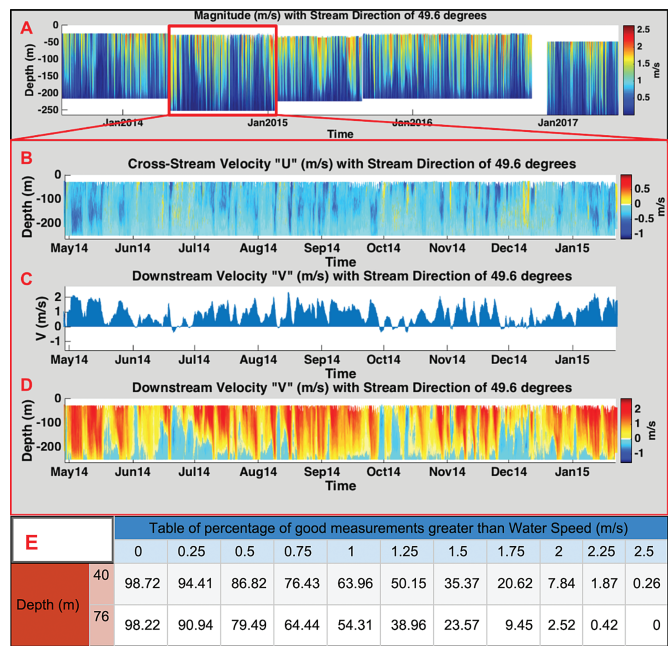
The Richardson number profile is shown in Figure 4D, with a vertical line at $1/4$, a value indicative of shear necessary to mix the stratification (Mack & Schoeberlein, 2004).

150-kHz ADCP and CTD Mooring

A different streamwise velocity coordinate system was chosen for the current velocity measurements over the water column at one location from the fixed mooring. The streamwise velocity for the moored ADCP current record was chosen to be the principal axis of the hourly depth averaged velocity vector for a 45-month time series. Positive downstream is 40° from true north, and positive cross-stream is 90° clockwise to the downstream, or approximately offshore relative to the isobaths. The mean depth of the maximum current speed during the time series is 56 m

FIGURE 5

Water speed from 3 years and 9 months (A) of current measurements made from the NCROEP 150-kHz ADCP moorings (approximate location shown in Figure 1) with May 2014–January 2015 highlighted, the second deployment showing cross stream velocity “*u*” (B), direction of the maximum current (C), and downstream velocity “*v*” (D). Positive downstream is toward the northeast at 49°, positive. (E) Comparison of 3 years and 9 months of measured current speeds at different depths from the ADCP mooring location in Figure 1.



and the mode is 28 m, with the latter being the shallowest velocity measurement made from the ADCP mooring shown in Figure 1. Water depth varies slightly over the time series from a minimum of 224 m to a maximum of 260 m. Individual mooring deployments were not always at the same location because of the challenges inherent in deploying instruments in a high-current deep-water environment on the upper slope (Figure 5).

Results

MHK: Current Measurements and CTD Casts From Vessel Cross-Stream Vertical Section

In 2016, we began making current observations from the *R/V Neil Armstrong*. Several cross-stream

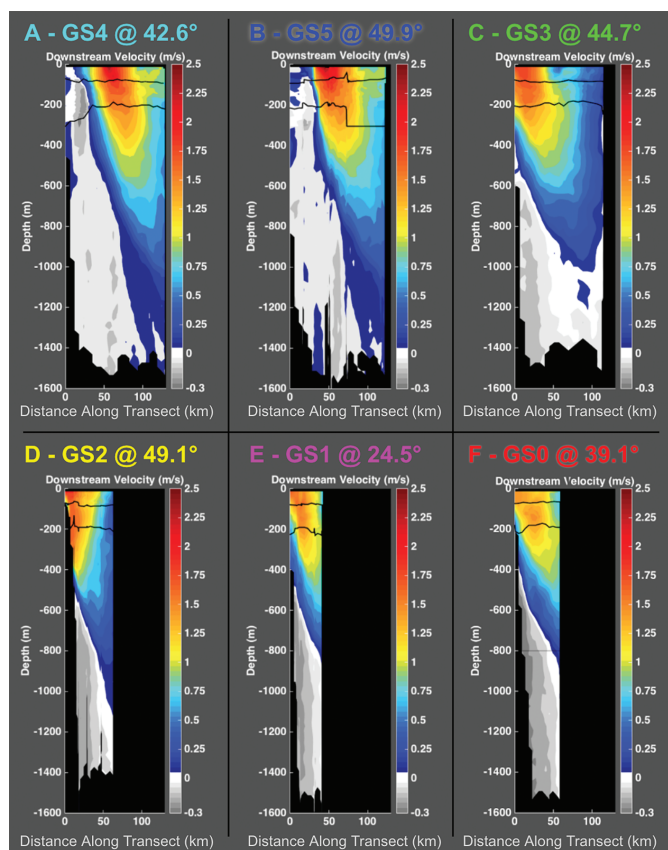
Several full water-column CTD casts were made during the *R/V Neil Armstrong* cruises. Vertical shear present where the ULSW flows counter to the GS is greatest beginning at a depth of 400 m beneath the GS jet, decreases in magnitude, and deepens offshore. Shears from the counterflow reach nearly the magnitude of those in the upper water column within the stream’s cyclonic shear zone (Figure 4B). Analysis of the current velocity (Figure 4A) and density structure at the cast locations provides valuable insights about the susceptibility of a mooring line or turbine to reversals in current direction, shear, and turbulence. The following are the results from further analysis of the observations made at the cast location shown in Figure 3. Recall the resolution for each instrument is 2, 5, and 20 m for the 300-, 150-, and 38-kHz ADCPs, respectively.

The greatest shears appear in the upper 200 m of the water column—in and beneath the jet—and again at the base of the stream, where the flow reverses from the northeastward stream flow to the ULSW in the upper limb of the DWBC, which is towards the south/southwest (Figure 4B). Quantifying the shear in these zones is essential for successful turbine and mooring development in the upper 200 m and for mooring design in deeper water.

The N^2 profiles (Figure 4C) show high stratification in the upper 200 m of the water column in the jet and again at depth where stream flow transitions to DWBC flow in the opposite direction. Note that the same zones that exhibit high stratification also exhibit higher shears. Furthermore, although there is much variability in the buoyancy frequency in these zones, the N^2 values for all

FIGURE 6

Current measurements made at the transects shown in Figure 2 from north to south, A–F. The label colors of each figure coincide with the transect color in Figure 2. Black contours mark transitions between different ADCPs; black areas are locations where data are not available. Cross-stream scales are the same for all figures.



three ADCPs agree. This is not the case with individual S^2 profiles from each ADCP, a point investigated further in the discussion.

Where the Richardson number is $\frac{1}{4}$ or less, the velocity shear is significant enough to provide the necessary conditions for mixing to occur in the water column. Indeed, Richardson numbers less than 1 have been shown to provide the necessary conditions to induce mixing in the Subtropical Atlantic (Mack & Schoeberlein, 2004). Note that this occurs both in the top 100-m surface layer and in the transition zone between the GS and ULSW (Figure 4D), between depths of 400–600 m (Andres et al., 2017).

150-kHz ADCP and CTD Mooring

The percentage of exceedance for different speeds from the first 3 years and 9 months of mooring measurements, at 40 and 76 m below the surface, is given in Figure 5E. The depths were chosen for comparison because they are potentially viable water column locations for a turbine and to contrast the difference in the frequency of occurrence of current speeds between 1 and 2 m/s at both depths. Previous analysis by Bane et al. (2017) focused only on 76 m below the surface.

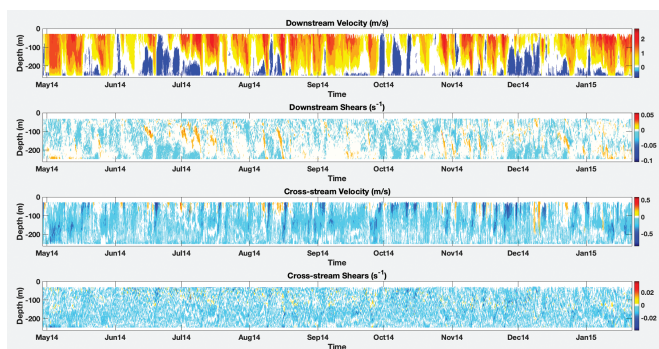
The currents exhibit much variability at the mooring location in Figure 1 as the GS meanders over the mooring and back offshore. A consid-

erable amount of vertical shear during times when the currents exceed 2 m/s is also apparent in the current speeds. Note the high percentage of the time when current speeds are less than 1 m/s. Slower current speeds over the mooring are likely the result of frequent meander passages that occur with a period of 3–8 days (Savidge, 2004), and GS path shifts that position of the GS offshore of the mooring for a week or more (Figure 5). Focusing on the second mooring deployment time series, outlined in red in Figure 5, several flow reversals are notable during the 9 months, with the first occurrence in June 2014 and several thereafter including three in October 2014 (Figure 5C). Most of these occurrences exhibit shoreward cross-stream current and near-zero or reversal, south/southwest flow, of the downstream current. These instances likely accompany the existence of a meander trough offshore of the mooring.

The vertical shear in the downstream and cross-stream directions, v/z and u/z , respectively, for the second ADCP deployment are shown in Figure 7, subplots 2 and 4 from top to bottom, respectively, along with downstream and cross-stream velocities. The magnitudes of shear maxima in the downstream direction from the mooring agree with the magnitudes of the downstream shear maxima seen in the vessel transect in Figure 3. The currents and shears seen during the second deployment have many notable events. Early in May, when downstream and onshore cross-stream velocities are both high throughout the entire water column (Figure 7), large positive downstream and onshore shears occur close to the bottom. The kinematics likely coincide with meander crest incursions over the mooring and repeat several times over the time series.

FIGURE 7

Downstream and cross-stream velocities and shears during the second mooring deployment from May 2014 to January 2015.



During periods when downstream currents approach 2 m/s in the top half of the water column, like the first week of July, downstream and offshore cross-stream shear maxima are apparent mid-water column. This occurs when the downstream direction is very close to the mean of 40°. Flow reversals that occur when the stream is offshore of the mooring, like those seen in October in the feather plot in Figure 5C, coincide

several occasions during the month. Also, note the character of the current during the flow reversal events on November 3, 16, and 27–29. During the reversal, the current veers from the mean northeastward direction to a south/southwestward flow of about 50 cm/s. The flow reversal likely results from the cyclonic circulation associated with the inshore side of a passing meander trough (Brooks & Bane, 1983). This is also evident in the strong onshore currents that precede the flow reversal on November 3, indicative of the approach of a meander trough. The reversal events around November 16 and 28 are not as pronounced, with lesser negative downstream speeds relative to the November 3 event and less pronounced onshore currents.

The mean velocities and shears for each ADCP mooring deployment time series are shown in Figure 9. Downstream velocities have a gradual nearly linear decrease from near surface to bottom. Cross-stream velocities vary significantly by deployment with cross-stream means for Deployments 3 and 5 being positive and negative for Deployments 1, 2, and 4. Note the inflection point in the cross-stream velocities that exists for all deployments beneath about 75 m. Although the bottom moorings are not all deployed at the same depth, with depths ranging from 220 to 265 m, they do have consistent downstream velocity and shear profiles. The largest downstream velocity means are seen in Deployment 3. Deployment 3 also has the largest offshore cross-stream mean velocity near the surface. Two downstream shear maxima are present in all deployment means, one at the base of the jet at a depth of about 100 m and another sometimes larger secondary maxima between 200 and

FIGURE 8

ADCP observations from November 2014 from top to bottom: downstream direction for the maximum velocity vector with the red line being the mean of 40° from true north, cross-stream velocity as a function of depth and time, top ADCP bin velocity vector, and the downstream velocity as a function of depth and time.

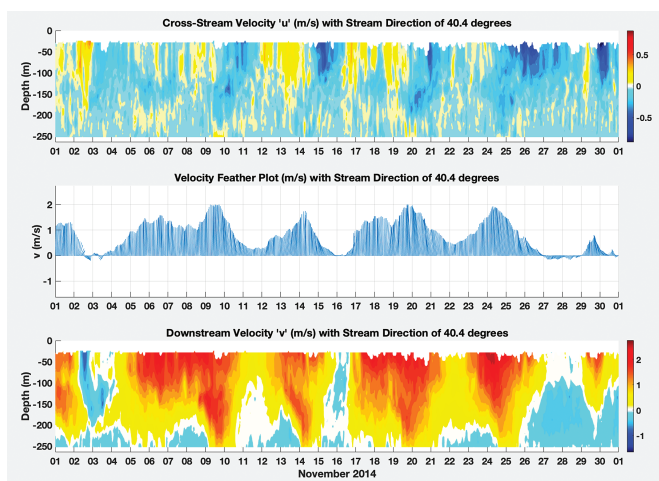
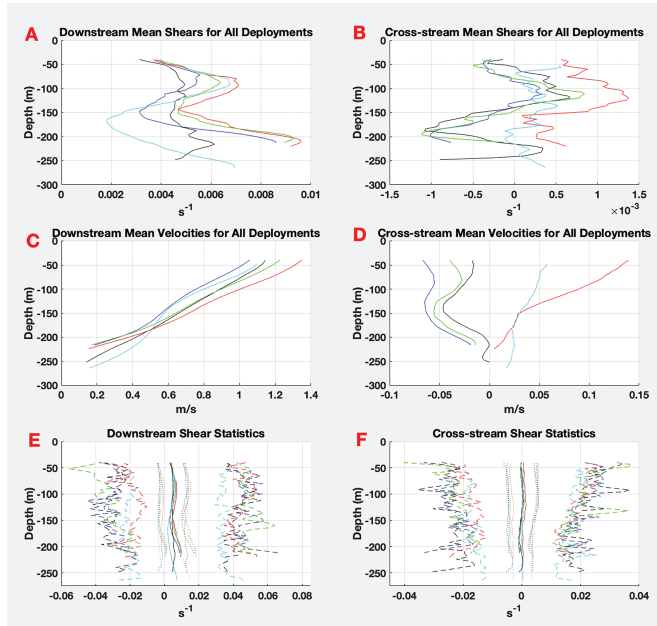


FIGURE 9

(A–D) Mean downstream and cross-stream velocities and shears for each ADCP mooring deployment. Deployments 1–5 are blue, black, red, green, and cyan, respectively. Deployment 5 (cyan) is the deepest in a water depth of 260 m. (E–F) Mean downstream (left) and cross-stream (right) shear profiles for the five ADCP deployments. The curve in the middle is the mean, the dotted curves on either side are ± 1 SD from the mean, and the outer curves are the maxima and minima for each deployment time series.



250 m. The largest shoreward and off-shore cross-stream mean velocities occur 50 m below the surface for three-fifths of the deployments, with Deployments 2 and 4 being the exceptions having half the mean shoreward current speeds at that depth. Cross-stream shears have two speed minima between about 50 and 100 m, and another beneath 150 m, with most having smaller minima at depth. The deepest deployment, the fifth, is an exception. There is an inflection point in the cross-stream shear profile that exists between 100 and 150 m for all deployments.

Cape Hatteras Transect velocity profiles, despite being nearly instantaneous velocity measurements rather than long-term means, demonstrate the same character as the long-term velocity and shear means seen in the mooring measurements. The Cape

Hatteras Transect (Figure 3A) has a shoreward cross-stream velocity on the inshore side of the transect at the depths of the moorings. The center panel, v/z , in Figure 3B exhibits two downstream shear maxima beneath the jet and closer to the bottom at the mooring depth.

The same mean downstream and cross-stream shears from the middle subplot in Figure 3 are shown below in Figure 9, with plots including ± 1 SD and their associated maxima and minima for each mooring deployment. The standard deviation for the downstream is nearly twice that for the cross-stream, 7.9×10^{-3} versus $4.3 \times 10^{-3} s^{-1}$. The depth averaged mean shear for all deployments is $4.7 \times 10^{-3} s^{-1}$ and $2.3 \times 10^{-4} s^{-1}$ in the downstream and cross-stream, respectively. Furthermore, the mean shear maxima of the downstream are

more than twice that of the cross-stream, $4.9 \times 10^{-2} s^{-1}$ versus $2.4 \times 10^{-2} s^{-1}$.

Discussion

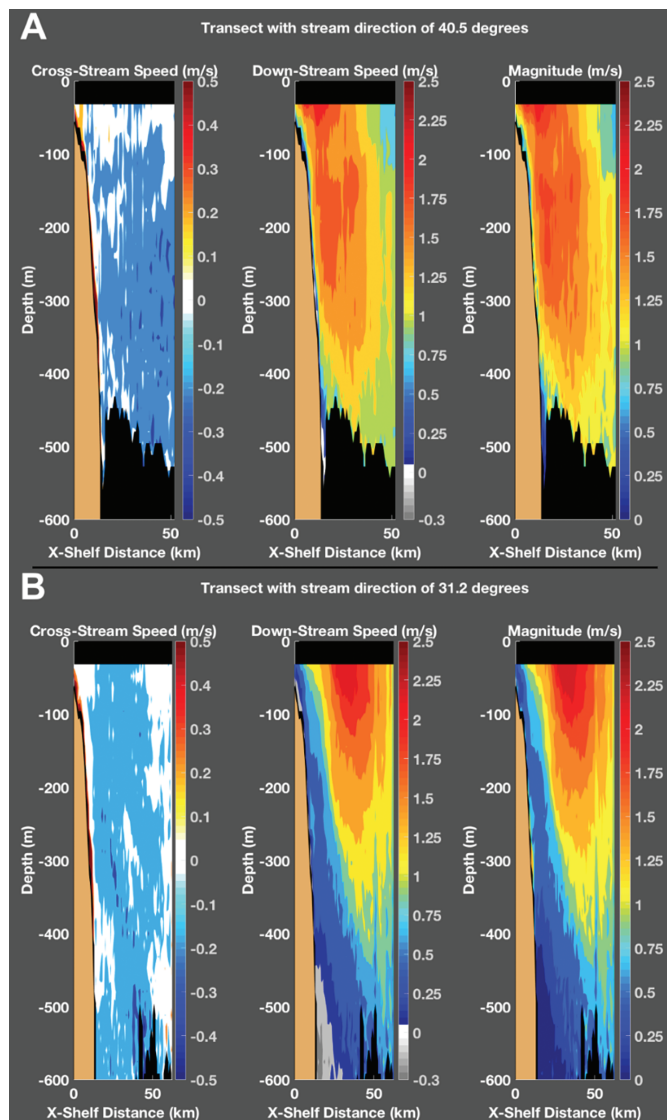
The observations presented herein provide several valuable insights about GS dynamics off Cape Hatteras and inform the MHK community considering engineering solutions for energy extraction in this region. They also begin to explore phenomena seen here for the first time.

Oceanography

The vessel transects made off Cape Hatteras provide several insights about the GS variability in velocity structure off Cape Hatteras, flow of ULSW south of the cape, potential instabilities caused by shearing in the stream and where the stream meets the ULSW at depth, and the potential existence of internal waves. Repeated measurements along the Cape Hatteras Line demonstrate that the velocity structure may vary along the same transect depending on whether the stream lies along the continental slope or offshore of it. The GS “wiggly garden hose” analogy provided in Halkin and Rossby (1985) may not be germane here where the stream regularly interacts with the continental margin. Along the Cape Hatteras Line, cross-stream vessel transects suggest the velocity structure may be quite different when the stream abuts the shelf break relative to instances when it is more offshore (Figure 10). Figure 10 shows the currents measured by *Miss Caroline*’s 75-kHz ADCP on separate dates along the Cape Hatteras Transect. The deepening of currents above 1 m/s by about 100 m in Figure 10A, when the current abuts the continental margin, is strikingly different from those in Figure 10B. Also, the skewing of higher

FIGURE 10

Velocity structure of the GS on the Cape Hatteras Line when it abutted the shelf break on February 20, 2018 (A), and when the GS was offshore of the continental margin on February 27, 2018 (B).



currents toward the shelf break is more apparent in Figure 10A, with current structure in Figure 10B tending to be more symmetric.

Flow of ULSW past Cape Hatteras was not thought to continue south of Cape Hatteras prior to the observations made in the vessel transects presented here and in Andres et al. (2017). Rather, the lower potential density ULSW first seen in SVC1 as a continuous southwestward flow be-

been measured on three separate cruises, and from two different vessels, along the Cape Hatteras transect to date: in March 2016, May 2017, August 2018, and November 2018 and from several glider cross-sections south of Cape Hatteras (Heiderich & Todd, 2020).

Velocity shear where ULSW passes beneath the stream can reach the same magnitude as that seen in the upper 200 m of the water column in the GS jet. An increase in thermal wind shear caused by the difference in potential density across sloping isopycnals between the GS and ULSW may contribute to the high shear between 400 and 600 m. From vessel velocity measurements and CTD casts, two zones were identified where both high shear and stratification exist simultaneously, and the Richardson number approaches a value low enough to promote turbulent mixing of the stratification: one between 50 and 200 m beneath the jet and the other where stream water meets ULSW between 400 and 600 m.

The rich current measurements made at the mooring site over 3 years and 9 months provide the longest time series of current measurements available at this location. The shear maxima that exist beneath 150 m in both the downstream and cross-stream currents demonstrate the influence of frequent meanders over the mooring, with the strong shoreward cross-shelf velocity component means suggesting the mooring was influenced often by stream meanders. The agreement between Deployments 1, 2, and 4, and the discrepancy between them and Deployments 3 and 5, with the latter two having lower cross-stream velocities and shear beneath 150 m, is worth consideration. Deployment 5 is the deepest mooring depth at ~265 m,

yet the means agree well with Deployment 3, which is in 224 m of water, both having the largest downstream velocity, and smallest cross-stream velocity means near the surface suggest these deployments spent more time in the jet, with less influence from meanders. Meander trough approaches are led by significant increases in cross-stream velocity and increased shear in the water column. The difference in mean cross-stream velocity during Deployments 3 and 5 relative to the other three deployments may be indicative of GS path shifts caused by interannual variability that is not yet well understood.

MHK

All of the aforementioned oceanographic dynamics discussed also provide valuable information to the engineering community considering MHK development. The vessel transects and CTD casts are valuable for optimizing the depth of mooring locations based on available MHK current resource, velocity and shear characterization, and water column stability. The effects of the enhanced velocity shear from unresolved small-scale shear on moorings require more observations, like lowering a higher frequency ADCP on a cast through this zone (Visbeck, 2002). The high shears between 400 and 600 m where the base of the stream meets the counterflow of the ULSW may be greater than that measured and is already significant for mooring design consideration at these depths. Shear magnitudes in the downstream direction from the mooring are more than twice those seen in the vessel transects in deeper waters. The transects do show shears of up to $\sim 0.03 \text{ s}^{-1}$ up on the shelf in the vicinity of the mooring, while downstream shear

maxima in the mooring are $\sim 0.04 \text{ s}^{-1}$, suggesting the highest shears are caused by the interaction of the high GS currents with the bottom. These agree with shear maxima seen in the mooring current measurements. Long-term currents measured by the mooring help to characterize the expected resource in greater detail than previously available. A comparison between the velocity available at 40 and 75 m below the surface from the long mooring time series elucidates the expected differences in the available MHK resource at different depths—an important consideration for optimizing turbine location in the water column. About a 10% greater occurrence of exceedance for speeds between 1 and 1.75 m/s exists between the two depths. Turbines located closer to the surface will necessarily require engineering to withstand the higher stresses caused by greater exposure to the surface wave field to take advantage of the greater resource. The frequent current rotations and flow reversals caused by the passage of meander troughs seen in the moored measurements will add increased torques to turbines here, and moorings will not exist as simple catenaries but as more complicated profiles with depth that will necessitate thoughtful engineering solutions. Additionally, the means from the mooring time series characterize the expected velocity shear in the water column and quantify maximum velocity and shear experienced by any device at this location. The long-term mean cross-shelf velocities are all shoreward, with shear maxima at depths greater than 150 m (Figure 9). Also notable are the maxima and minima for the long-term mooring mean shears—about an order of magnitude greater than the mean values, up to 0.06 s^{-1}

for the downstream and 0.04 s^{-1} for the cross-stream.

Summary and Future Work

Detailed observations have been presented that provide in-situ views of the velocity structure in the GS off Cape Hatteras, NC. They quantify spatial and temporal variability in the velocity and baroclinic structure along the Cape Hatteras Line and provide a necessary basis for future MHK or even traditional utility development in the area.

Several vessel crossings of the Cape Hatteras Transect demonstrate the difference in velocity structure when the GS flows closer to the shelf break or is offshore of it. They quantify shearing, stratification, and water column stability from current measurements and CTD casts along the Cape Hatteras Transect and identify new features at this location like the possibly persistent ULSW flow beneath the stream and near inertial internal waves.

Analyses of a 3-year-and-9-month time series of current, salinity, and temperature measurements from a mooring that contains a 150-kHz ADCP were presented that summarize the exceedance of currents at specific speeds at depths of 40 and 75 m below the surface for future device design consideration. The measured currents show the influence of frequent GS meander propagation and path shifts over the mooring that produce flow reversals and strong shears throughout the water column. Downstream and cross-stream velocities as well as long-term means demonstrate the persistent shoreward flow at the mooring that may be caused

by the frequent approach of mean-
der troughs. Several specific occur-
rences were noted for the month of
November 2014.

The observations presently sup-
port several collaborative and con-
tinuing engineering efforts on
turbine, kite, and mooring design
(Bin-Karim et al., 2018; Divi et al.,
2017), economic assessment of GS
MHK (Li et al., 2017; Neary et al.,
2014), subsurface ADCP mooring
design with National Oceanic and At-
mospheric Administration's Center
for Operational Products and Services
division, and research with Dr. Lind-
say Dubb's group (Coastal Studies In-

stitute, 2020) to understand marine
mammal abundance relative to GS
variability off Cape Hatteras. Future
work will use hourly HF radar surface
velocity measurements in conjunction
with the moored ADCP currents to
provide detailed examination and
analysis of GS meander propagation
at the mooring site. Further analysis
of CTD and ADCP observations
may enhance understanding of the
complex interplay between shelf
water masses of the South Atlantic
Bight, Mid-Atlantic Bight, and Slope
Sea, as well as deeper waters down the
continental slope like the ULSW,
with GS variability. Observations
also identify new phenomena that
warrant further research like the po-
tentially persistent flow of ULSW be-
neath the GS (Andres et al., 2017;
Heiderich & Todd, 2020), variability
in GS velocity structure dependence
on stream location relative to the con-
tinental margin, and the effects of un-
resolved small-scale shear on the shear
profiles within and beneath the
stream, as well as their influence on
important exchange processes like
CO₂ fluxes at strong mixing zones be-
tween differing water masses and ex-

Acknowledgments

The authors would like to thank
the North Carolina Renewable
Ocean Energy Program and the Na-
tional Science Foundation Processes
Driving Exchange at Cape Hatteras
(PEACH) program for supporting
these observations. They would also
like to thank Sara Haines, John
Bane, and Nick DeSimone and the
crew of the RV *Neil Armstrong*.

Corresponding Author:

Michael Muglia
ECU Coastal Studies Institute
850 NC 345, Wanchese, NC 27981
Email: mugliam@ecu.edu

References

- Andres, M. 2016. On the recent destabilization of the Gulf Stream path downstream of Cape Hatteras. *Geophys Res Lett.* 43(18):9836-42. <https://doi.org/10.1002/2016GL069966>.
- Andres, M., Muglia, M., Bahr, F., & Bane, J. 2018. Continuous flow of upper Labrador Seawater around Cape Hatteras. *Sci Rep-UK.* 8(1):1-8. <https://doi.org/10.1038/s41598-018-22758-z>.
- Bane, J.M., He, R., Muglia, M., Lowcher, C.F., Gong, Y., & Haines, S.M. 2017. Marine hydrokinetic energy from western boundary currents. *Annu Rev Mar Sci.* 9:105-23. <https://doi.org/10.1146/annurev-marine-010816-060423>.
- Bane, J.M., Jr., Brooks, D.A., & Lorenson, K.R. 1981. Synoptic observations of the three-dimensional structure and propagation of Gulf Stream meanders along the Carolina continental margin. *J Geophys Res-Oceans.* 86(C7):6411-25. <https://doi.org/10.1029/JC086iC07p06411>.
- Bane, J.M., Jr., & Dewar, W.K. 1988. Gulf Stream bimodality and variability downstream of the Charleston Bump. *J Geophys Res-Oceans.* 93(C6):6695-710. <https://doi.org/10.1029/JC093iC06p06695>.
- Bin-Karim, S., Muglia, M., Mazzoleni, A., & Vermillion, C. 2018. Control of a relocatable energy-harvesting autonomous underwater vehicle in a spatiotemporally-varying Gulf Stream resource. In: 2018 Annual American Control Conference (ACC), pp. 2575-80. Milwaukee, WI: IEEE. <https://doi.org/10.23919/ACC.2018.8431318>.
- Bower, A.S., & Rossby, T. 1989. Evidence of cross-frontal exchange processes in the Gulf Stream based on isopycnal RAFOS float data. *J Phys Oceanogr.* 19(9):1177-90. [https://doi.org/10.1175/1520-0485\(1989\)019<1177:EOCFEP>2.0.CO;2](https://doi.org/10.1175/1520-0485(1989)019<1177:EOCFEP>2.0.CO;2).
- Brooks, D.A., & Bane, J.M. 1983. Gulf Stream meanders off North Carolina during winter and summer 1979. *J Geophys Res-Oceans.* 88(C8):4633-50. <https://doi.org/10.1029/JC088iC08p04633>.
- Chen, K., & He, R. 2010. Numerical investigation of the Middle Atlantic Bight shelfbreak frontal circulation using a high-resolution ocean hindcast model. *J Phys Oceanogr.* 40(5):949-64. <https://doi.org/10.1175/2009JPO4262.1>.
- Divi, S., Tandon, S., & Mazzoleni, A. 2017. Conceptual design and feasibility analysis of a mobile underwater turbine system for harvesting Gulf-Stream marine hydrokinetic energy. *Renew Energ.*
- Coastal Studies Institute. 2020. Environmental and regulatory assessment. Available at: <https://www.coastalstudiesinstitute.org/research/coastal-engineering/renewable-ocean-energy-project-overview/environmental-and-regulatory-assessment/>. (accessed 22 June 2020).
- Flagg, C.N., Pietrafesa, L.J., & Weatherly, G.L. 2002. Springtime hydrography of the southern Middle Atlantic Bight and the onset of seasonal stratification. *Deep-Sea Res Pt II.* 49(20):4297-329. [https://doi.org/10.1016/S0967-0645\(02\)00121-2](https://doi.org/10.1016/S0967-0645(02)00121-2).
- General Assembly of North Carolina. 2012. An Act to Modify the Current Operations and Capital Improvements Appropriations Act of

- 2009 and for Other Purposes. Session Law 1146 2010-31, Senate Bill 897. Session 2009. 1147 H. Rept. 131, pt. 1. Washington, DC: GPO, 1148 2001. The Library of Congress, Thomas. 1149
- Glenn, S.M., & Ebbesmeyer, C.C.** 1994. 1150 Observations of Gulf Stream frontal eddies 1151 in the vicinity of Cape Hatteras. *J Geophys* 1152 *Res-Oceans*. 99(C3):5047-55. [https://doi.](https://doi.org/10.1029/93JC02787) 1153 [org/10.1029/93JC02787](https://doi.org/10.1029/93JC02787). 1154
- Gula, J., Molemaker, M.J., & McWilliams, J.C.** 2015. Gulf Stream dynamics along the 1155 southeastern US seaboard. *J Phys Oceanogr.* 1156 45(3):690-715. [https://doi.org/10.1175/](https://doi.org/10.1175/JPO-D-14-0154.1) 1157 [JPO-D-14-0154.1](https://doi.org/10.1175/JPO-D-14-0154.1). 1158
- Haines, S., Seim, H., & Muglia, M.** 2017. 1159 Implementing quality control of high-frequency 1160 radar estimates and application to Gulf 1161 Stream surface currents. *J Atmos Ocean* 1162 *Tech.* 34(6):1207-24. [https://doi.org/10.1175/](https://doi.org/10.1175/JTECH-D-16-0203.1) 1163 [JTECH-D-16-0203.1](https://doi.org/10.1175/JTECH-D-16-0203.1). 1164
- Halkin, D., & Rossby, T.** 1985. The structure 1165 and transport of the Gulf Stream at 73 W. 1166 *J Phys Oceanogr.* 15(11):1439-52. [https://doi.](https://doi.org/10.1175/1520-0485(1985)015<1439:TSATOT>2.0.CO;2) 1167 [org/10.1175/1520-0485\(1985\)015<1439:](https://doi.org/10.1175/1520-0485(1985)015<1439:TSATOT>2.0.CO;2) 1168 [TSATOT>2.0.CO;2](https://doi.org/10.1175/1520-0485(1985)015<1439:TSATOT>2.0.CO;2). 1169
- Hall, M.M., & Bryden, H.L.** 1985. Profiling 1170 the Gulf Stream with a current meter moor- 1171 ing. *Geophys Res Lett.* 12(4):203-6. [https://](https://doi.org/10.1029/GL012i004p00203) 1172 doi.org/10.1029/GL012i004p00203. 1173
- Heiderich, J., & Todd, R.E.** 2020. Along- 1174 stream evolution of Gulf Stream volume 1175 transport. *J Phys Oceanogr.* 50(8):2251-70. 1176 <https://doi.org/10.1175/JPO-D-19-0303.1>. 1177
- Hogg, N.G.** 1992. On the transport of the 1178 Gulf Stream between Cape Hatteras and the 1179 Grand Banks. *Deep-Sea Res.* 39(7-8):1231-46. 1180 [https://doi.org/10.1016/0198-0149\(92\)](https://doi.org/10.1016/0198-0149(92)90066-3) 1181 [90066-3](https://doi.org/10.1016/0198-0149(92)90066-3). 1182
- Johns, W.E., Shay, T.J., Bane, J.M., & Watts, D.R.** 1995. Gulf Stream structure, transport, 1183 and recirculation near 68 W. *J Geophys Res-* 1184 *Oceans.* 100(C1):817-38. [https://doi.org/10.](https://doi.org/10.1029/94JC02497) 1185 [1029/94JC02497](https://doi.org/10.1029/94JC02497). 1186
- Li, B., de Queiroz, A.R., DeCarolis, J.F., Bane, J., He, R., Keeler, A.G., & Neary, V.S.** 2017. The economics of electricity generation 1187 1188 1189 1190 1191 from Gulf Stream currents. *Energy.* 134:649-58. 1192 <https://doi.org/10.1016/j.energy.2017.06.048>. 1193
- Lowcher, C.F., Muglia, M., Bane, J.M., He, R., Gong, Y., & Haines, S.M.** 2017. Marine 1194 hydrokinetic energy in the Gulf Stream off 1195 North Carolina: An assessment using obser- 1196 vations and ocean circulation models. In: *Marine* 1197 *Renewable Energy*, eds. Yang, Z., & Copping, 1198 A., pp. 237-58. Cham, Switzerland: Springer. 1199 [https://doi.org/10.1007/978-3-319-53536-](https://doi.org/10.1007/978-3-319-53536-1202_4_10) 1200 [1202_4_10](https://doi.org/10.1007/978-3-319-53536-1202_4_10). 1201
- Mack, S.A., & Schoeberlein, H.C.** 2004. Rich- 1202 ardson number and ocean mixing: Towed chain 1203 observations. *J Phys Oceanogr.* 34(4):736-54. 1204 [https://doi.org/10.1175/1520-0485\(2004\)](https://doi.org/10.1175/1520-0485(2004)034<0736:RNAOMT>2.0.CO;2) 1205 [034<0736:RNAOMT>2.0.CO;2](https://doi.org/10.1175/1520-0485(2004)034<0736:RNAOMT>2.0.CO;2). 1206
- Meinen, C.S., Luther, D.S., & Baringer, M.O.** 2009. Structure, transport and potential vor- 1207 ticity of the Gulf Stream at 68 W: Revisiting 1208 older data sets with new techniques. *Deep-Sea* 1209 *Res Pt I.* 56(1):41-60. [https://doi.org/10.1016/](https://doi.org/10.1016/j.dsr.2008.07.010) 1210 [j.dsr.2008.07.010](https://doi.org/10.1016/j.dsr.2008.07.010). 1211
- Miller, J.L.** 1994. Fluctuations of Gulf Stream 1212 frontal position between Cape Hatteras and 1213 the Straits of Florida. *J Geophys Res-Oceans.* 99(C3):5057-64. [https://doi.org/10.1029/](https://doi.org/10.1029/93JC03484) 1214 [93JC03484](https://doi.org/10.1029/93JC03484). 1215
- Nagai, T., Tandon, A., Kunze, E., & Mahadevan, A.** 2015. Spontaneous generation of near-inertial 1216 waves by the Kuroshio Front. *J Phys Oceanogr.* 45(9):2381-406. [https://doi.org/10.1175/](https://doi.org/10.1175/JPO-D-14-0086.1) 1217 [JPO-D-14-0086.1](https://doi.org/10.1175/JPO-D-14-0086.1). 1218
- Neary, V.S., Lawson, M., Previsic, M., Copping, A., Hallett, K.C., LaBonte, A., & Murray, D.** 2014. Methodology for Design and Economic 1219 Analysis of Marine Energy Conversion (MEC) 1220 Technologies (No. SAND2014-3561C). 1221 Albuquerque, NM: Sandia National Lab 1222 (SNL-NM). 1223
- Pickart, R.S., & Smethie, W.M., Jr.** 1993. How does the deep western boundary current 1224 cross the Gulf Stream? *J Phys Oceanogr.* 23(12):2602-16. [https://doi.org/10.1175/](https://doi.org/10.1175/1520-0485(1993)023<2602:HDTDWB>2.0.CO;2) 1225 [1520-0485\(1993\)023<2602:HDTDWB>2.0.](https://doi.org/10.1175/1520-0485(1993)023<2602:HDTDWB>2.0.CO;2) 1226 [CO;2](https://doi.org/10.1175/1520-0485(1993)023<2602:HDTDWB>2.0.CO;2). 1227
- Rainville, L., & Pinkel, R.** 2004. Observations of energetic high-wavenumber internal waves in the 1228 Kuroshio. *J Phys Oceanogr.* 34(7):1495-505. 1229 [https://doi.org/10.1175/1520-0485\(2004\)](https://doi.org/10.1175/1520-0485(2004)034<1495:OOEHIW>2.0.CO;2) 1230 [034<1495:OOEHIW>2.0.CO;2](https://doi.org/10.1175/1520-0485(2004)034<1495:OOEHIW>2.0.CO;2). 1231
- Richardson, P.L.** 1977. On the crossover between the Gulf Stream and the Western Boundary Undercurrent. *Deep-Sea Res.* 24(2):139-59. 1232 [https://doi.org/10.1016/0146-6291\(77\)](https://doi.org/10.1016/0146-6291(77)90549-5) 1233 [90549-5](https://doi.org/10.1016/0146-6291(77)90549-5). 1234
- Savidge, D.K.** 2004. Gulf stream meander propagation past Cape Hatteras. *J Phys Oceanogr.* 34(9):2073-85. [https://doi.](https://doi.org/10.1175/1520-0485(2004)034<2073:GSMPPC>2.0.CO;2) 1235 [org/10.1175/1520-0485\(2004\)034<2073:](https://doi.org/10.1175/1520-0485(2004)034<2073:GSMPPC>2.0.CO;2) 1236 [GSMPPC>2.0.CO;2](https://doi.org/10.1175/1520-0485(2004)034<2073:GSMPPC>2.0.CO;2). 1237
- Savidge, D.K., & Savidge, W.B.** 2014. Seasonal export of South Atlantic Bight and Mid-Atlantic Bight shelf waters at Cape Hatteras. 1238 *Cont Shelf Res.* 74:50-59. [https://doi.org/](https://doi.org/10.1016/j.csr.2013.12.008) 1239 [10.1016/j.csr.2013.12.008](https://doi.org/10.1016/j.csr.2013.12.008). 1240
- Tracey, K.L., & Watts, D.R.** 1986. On Gulf stream meander characteristics near Cape Hatteras. 1241 *J Geophys Res-Oceans.* 91(C6):7587-602. 1242 <https://doi.org/10.1029/JC091iC06p07587>. 1243
- Visbeck, M.** 2002. Deep velocity profiling using lowered acoustic Doppler current profilers: Bottom track and inverse solutions. 1244 *J Atmos Ocean Tech.* 19(5):794-807. 1245 [https://doi.org/10.1175/1520-0426\(2002\)](https://doi.org/10.1175/1520-0426(2002)019<0794:DVPULA>2.0.CO;2) 1246 [019<0794:DVPULA>2.0.CO;2](https://doi.org/10.1175/1520-0426(2002)019<0794:DVPULA>2.0.CO;2). 1247
- Watts, D.R., Tracey, K.L., Bane, J.M., & Shay, T.J.** 1995. Gulf Stream path and thermocline structure near 74 W and 68 W. *J Geophys Res-Oceans.* 100(C9):18291-18312. [https://doi.](https://doi.org/10.1029/95JC01850) 1248 [org/10.1029/95JC01850](https://doi.org/10.1029/95JC01850). 1249
- Winkel, D.P., Gregg, M.C., & Sanford, T.B.** 2002. Patterns of shear and turbulence across the Florida Current. *J Phys Oceanogr.* 32(11):3269-85. [https://doi.org/10.1175/](https://doi.org/10.1175/1520-0485(2002)032<3269:POSATA>2.0.CO;2) 1250 [1520-0485\(2002\)032<3269:POSATA>2.0.](https://doi.org/10.1175/1520-0485(2002)032<3269:POSATA>2.0.CO;2) 1251 [CO;2](https://doi.org/10.1175/1520-0485(2002)032<3269:POSATA>2.0.CO;2). 1252

AUTHOR QUERIES

AUTHOR PLEASE ANSWER QUERIES

- Q1: Please provide city and state/country location for this affiliation (ECA Coastal Studies Institute).
- Q2: Please check whether “+–” should be “±.”
- Q3: Andres et al., 2017, is missing from the reference list. Please provide reference details or remove the reference from the text.
- Q4: Hogg, 1991, is missing from the reference list. Please provide reference details or remove the reference from the text.
- Q5: Bane & Brooks, 1979, is missing from the reference list. Please provide reference details or remove the reference from the text.
- Q6: Andres et al., 2016, is missing from the reference list. Please provide reference details or remove the reference from the text.
- Q7: Lowcher et al., 2014, is missing from the reference list. Please provide reference details or remove the reference from the text.
- Q8: Please cite this reference (Andres, 2016) in the text or confirm if it should be deleted.
- Q9: Please cite this reference (Andres et al., 2018) in the text or confirm if it should be deleted.
- Q10: Please cite this reference (Bane et al., 1981) in the text or confirm if it should be deleted.
- Q11: Please cite this reference (Bower & Rossby, 1989) in the text or confirm if it should be deleted.
- Q12: Please provide volume and page numbers for this reference (Divi et al., 2017).
- Q13: Please check whether the details of this reference (General Assembly of North Carolina, 2012) were correctly captured.
- Q14: Please cite this reference (Gula et al., 2015) in the text or confirm if it should be deleted.
- Q15: Please cite this reference (Haines et al., 2017) in the text or confirm if it should be deleted.
- Q16: Please cite this reference (Lowcher et al., 2017) in the text or confirm if it should be deleted.
- Q17: Please cite this reference (Nagai et al., 2015) in the text or confirm if it should be deleted.
- Q18: Please cite this reference (Rainville & Pinkel, 2004) in the text or confirm if it should be deleted.
- Q19: Please cite this reference (Richardson, 1977) in the text or confirm if it should be deleted.
- Q20: Please cite this reference (Savidge & Savidge, 2014) in the text or confirm if it should be deleted.

END OF AUTHOR QUERIES